

# Oxygen-Generating Photo-Cross-Linkable Hydrogels Support Cardiac Progenitor Cell Survival by Reducing Hypoxia-Induced Necrosis

Neslihan Alemdar,<sup>†,‡,§</sup> Jeroen Leijten,<sup>†,‡,§</sup> Gulden Camci-Unal,<sup>†,‡,^</sup> Jesper Hjortnaes,<sup>†,‡,||</sup> Joao Ribas,<sup>†,‡,@</sup> Arghya Paul,<sup>†,‡</sup> Pooria Mostafalu,<sup>‡</sup> Akhilesh K. Gaharwar,<sup>†,‡,◆</sup> Yiling Qiu,<sup>#</sup> Sameer Sonkusale,<sup>‡</sup> Ronglih Liao,<sup>#</sup> and Ali Khademhosseini<sup>\*,†,‡,▽,○,||</sup>

<sup>†</sup>Biomaterials Innovation Research Center, Department of Medicine, Brigham and Women's Hospital, Harvard Medical School, Cambridge, Massachusetts 02139, United States

<sup>‡</sup>Harvard-MIT Division of Health Sciences and Technology, Massachusetts Institute of Technology, 77 Massachusetts Avenue, Cambridge, Massachusetts 02139, United States

<sup>§</sup>Department of Developmental BioEngineering, MIRA Institute for Biomedical Technology and Technical Medicine, University of Twente, Enschede, The Netherlands

<sup>||</sup>Department of Cardiothoracic Surgery, University Medical Center Utrecht, Utrecht, Netherlands

<sup>‡</sup>Department of Electrical and Computer and Engineering, Tufts University, Medford Massachusetts 02155, United States

<sup>#</sup>Cardiac Muscle Research Laboratory, Department of Medicine, Brigham and Women's Hospital, Harvard Medical School, Boston, Massachusetts 02115, United States

<sup>▽</sup>Wyss Institute for Biologically Inspired Engineering, Harvard University, Boston, Massachusetts 02115, United States

<sup>○</sup>Department of Bioindustrial Technologies, College of Animal Bioscience and Technology, Konkuk University, Hwayang-dong, Gwangjin-gu, Seoul 143-701, Republic of Korea

<sup>||</sup>Department of Physics, King Abdulaziz University, Jeddah, 21569, Saudi Arabia

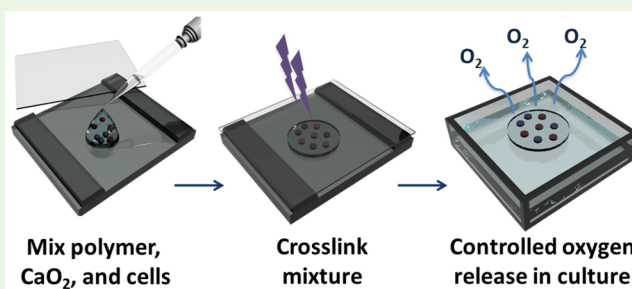
<sup>@</sup>Doctoral Program in Experimental Biology and Biomedicine, Center for Neuroscience and Cell Biology, Institute for Interdisciplinary Research, University of Coimbra, 3030-789 Coimbra, Portugal

## Supporting Information

**ABSTRACT:** Oxygen is essential to cell survival and tissue function. Not surprisingly, ischemia resulting from myocardial infarction induces cell death and tissue necrosis. Attempts to regenerate myocardial tissue with cell based therapies exacerbate the hypoxic stress by further increasing the metabolic burden. In consequence, implanted tissue engineered cardiac tissues suffer from hypoxia-induced cell death. Here, we report on the generation of oxygen-generating hydrogels composed of calcium peroxide (CPO) laden gelatin methacryloyl (GelMA). CPO-GelMA hydrogels released significant amounts of oxygen for over a period of 5 days under hypoxic conditions (1% O<sub>2</sub>).

The released oxygen proved sufficient to relieve the metabolic stress of cardiac side population cells that were encapsulated within CPO-GelMA hydrogels. In particular, incorporation of CPO in GelMA hydrogels strongly enhanced cell viability as compared to GelMA-only hydrogels. Importantly, CPO-based oxygen generation reduced cell death by limiting hypoxia-induced necrosis. The current study demonstrates that CPO based oxygen-generating hydrogels could be used to transiently provide oxygen to cardiac cells under ischemic conditions. Therefore, oxygen generating materials such as CPO-GelMA can improve cell-based therapies aimed at treatment or regeneration of infarcted myocardial tissue.

**KEYWORDS:** cell survival, implantation, avascular, tissue engineering, stem cells, controlled release, oxygen evolution, biomaterials



## INTRODUCTION

Ischemic heart disease occurs when cardiac tissue is deprived of oxygen, which leads to progressive functional loss and apoptosis of cardiac cells.<sup>1</sup> The permanent loss of function initiates a cascade of detrimental events, including the formation of a noncontractile scar, ventricular wall thinning, and subsequent progressive heart failure. Currently available pharmacotherapies fail to address the loss of functional cardiomyocytes. Restoring

damaged heart muscle tissue through stem cell based regeneration offers potential opportunities to treat heart failure.<sup>2,3</sup>

**Special Issue:** Tissue Engineering

**Received:** February 24, 2016

**Accepted:** April 25, 2016

**Published:** April 25, 2016

In particular, cardiac side population cells (CSPs), a distinct subpopulation of endogenous cardiac progenitor cells, have been shown to differentiate efficiently to all cell types in healthy myocardium, including functional mature cardiomyocytes.<sup>4–6</sup> Thus, CSPs offer tremendous prospect for cell therapy applications to promote cardiac regeneration post-myocardial injury. However, *in vivo* performances of such strategies are limited by the significant loss of implanted cells.<sup>7</sup> Although it is known that hypoxic oxygen tensions can be beneficial for the function of implanted cells, the anoxic stresses found in ischemic myocardial tissue cause massive loss of implanted cells.<sup>8–10</sup> In fact, the implanted cells or tissues are prevascular and thus rely on passive diffusion of oxygen from an ischemic tissue. This further increases the metabolic burden on the nutritionally impoverished tissue. Not surprisingly, implantation of cells into a metabolically deprived microenvironment leads to suboptimal therapeutic efficacies in myocardial therapy.<sup>11–13</sup>

Thus, developing strategies that enable the survival of transplanted CSPs in an ischemic microenvironment might represent a key stepping stone to improve medical outcomes. In particular, efficiently increasing the tissue's oxygen tension is expected to increase the early survival of transplanted CSPs. This would allow for the differentiation of CSPs into functional cardiomyocytes, which is expected to ultimately lead to improved cardiac performance of the infarcted heart.

A wide variety of strategies have been explored to improve the regeneration of myocardial tissue.<sup>14</sup> This includes genetic modification of stem cells,<sup>15–17</sup> cell preconditioning before transplantation,<sup>18</sup> biomaterials-based cell delivery approaches,<sup>19</sup> e.g., microencapsulation of cells, application of biopolymers,<sup>20</sup> nanoscaffolds,<sup>21,22</sup> cardiac patches,<sup>23</sup> nanowires,<sup>26</sup> and bio-compatible pro-angiogenic hydrogels.<sup>24–27</sup> Typically, these approaches have been reported to achieve initial vascularization 3 to 7 days post-implantation. However, none addressed the efficient supply of oxygen in the prevascular phase of the implant and thus are associated with hypoxia-induced cell death.

Designing hydrogels that produce oxygen in a controlled manner may offer a unique solution to prevent ischemia-induced death of implanted cells as well as control their cell fate.<sup>28,29</sup> Solid peroxides have been reported to controllably release oxygen in aqueous environments in amounts that are able to sustain cell survival under ischemic conditions.<sup>30–33</sup> Herein, we hypothesized that the incorporation of solid peroxides into biomaterials would yield an oxygen-generating three-dimensional (3D) cell microenvironment that allows CSP survival and minimizes tissue necrosis under ischemic conditions. To test this, CSPs and calcium peroxide (CPO) were laden into the photo-cross-linkable hydrogel gelatin methacryloyl (GelMA) and culturing the resulting tissue engineered implant under hypoxic conditions. Our earlier studies have shown the biocompatibility and biodegradability of GelMA for stem cell delivery and *in vivo* myocardial therapy.<sup>27,34–37</sup> Moreover, these hydrogels can be modulated on the microscale to induce stem cell differentiation into different lineages.<sup>38,39</sup> The current study demonstrates, for the first time, the potential of oxygen-generating GelMA hydrogels to maintain the survival of CSPs in a 3D microenvironment *in vitro* under hypoxic conditions to promote CSP-based myocardial therapy in ischemic conditions.

## MATERIALS AND METHODS

**Materials.** Gelatin (Type A, 300 bloom from porcine skin), methacrylic anhydride (MA), CPO, catalase (obtained from bovine liver, 2950 units/mg protein), L-glutamine, 3-(trimethoxysilyl) propyl methacrylate

(TMSPMA), Alizarin red S, and dimethyl sulfoxide (DMSO) were purchased from Sigma-Aldrich (St. Louis, MO, USA). The photoinitiator 2-hydroxy-1-[4-(hydroxyethoxy) phenyl]-2-methyl-1-propanone (Irgacure 2959) was obtained from BASF (Ludwigshafen, Germany). CSPs were obtained, with informed consent and approval of the local ethical committee, from Brigham and Women's Hospital (Boston, MA, USA). Dulbecco's phosphate buffered saline (DPBS), trypsin-EDTA, and penicillin–streptomycin were purchased from Gibco (USA). Alpha-modified Eagle's medium (Alpha-MEM) was supplied by Invitrogen (Grand Island, NY, USA). HyClone Characterized FBS and precleaned microscope slides were obtained from Fisher Scientific (Waltham, MA, USA). 3-(4,5-Dimethylthiazol-2-yl)-5-(3-carboxymethoxyphenyl)-2-(4-sulfophenyl)-2H-tetrazolium solution (MTS) was provided from Promega (USA). The live/dead viability/cytotoxicity kit was obtained from Invitrogen (Grand Island, NY, USA). Apoptotic/necrotic cell detection kit was purchased from PromoKine (USA). The UV source (Omnicure model S2000) was provided by EXPO Photonic Solutions Inc. (Ontario, Canada).

**Synthesis of GelMA.** GelMA was synthesized as described before.<sup>36</sup> First, gelatin was mixed at 10% (w/v) into DPBS at 50 °C. After the gelatin totally dissolved in DPBS, 8 mL of MA was added dropwise to this mixture at the same temperature. The reaction was carried out for 3 h at 50 °C. At the end of this process, the reaction mixture was diluted by DPBS to stop reaction. Then, the mixture was dialyzed using 12–14 kDa cutoff dialysis tubing in distilled water during 1 week at 40 °C to remove salts and unreacted methacrylic anhydride. The obtained solution was frozen at –80 °C and then freeze-dried for 1 week to form white porous GelMA foam and stored at –80 °C until further use.

**Fabrication of Oxygen-Generating CPO-GelMA Hydrogels.** GelMA was first dissolved in DMSO, and then CPO was added as an oxygen-generating agent at varying concentrations ranging from 0 to 3 wt % and mixed at room temperature by magnetic stirring to form a homogeneous solution (Table 1). GelMA samples containing CPO were then frozen at –80 °C and placed in a freeze-dryer for 3 days. 5% (w/v) CPO-GelMA solutions containing 0.1% (w/v) photoinitiator (Irgacure 2959) and CPO-GelMA were exposed to UV light (50 s at 2.5 mW/cm<sup>2</sup>) to form cross-linked hydrogels with a thickness of 450 μm (Figure 1A).

**CPO Distribution in GelMA.** To confirm homogeneous incorporation of CPO in GelMA, the cross-linked hydrogel samples were stained with Alizarin red S. For this purpose, 2% (w/v) Alizarin Red S solution was freshly prepared in distilled water and set to pH 4.2. GelMA was incubated with Alizarin Red S for 20 min, rinsed with DI water until the washing solution was clear, and microphotographed.

**CPO-GelMA Microstructure and Porosity.** The microstructures of CPO-GelMA hydrogels with different CPO concentrations were characterized by scanning electron microscopy (SEM). For SEM analyses, hydrogels without cells were cross-linked, immersed in liquid nitrogen, freeze-dried for 3 days, and gold coated. SEM images were taken using a SEM microscope (Gemini column Zeiss Supra 40VP Field Emission Scanning Electron Microscope) and analyzed on microstructure and porosity using image based analysis using ImageJ software.

**Water Uptake of Oxygen-Generating Hydrogels.** Hydrogels without cells were prepared as described previously, weighed, and immersed into DPBS at 37 °C for 24 h. The weight of the swollen samples was determined after the excess water on the surface of the gel was removed. The swelling ratio (SR) of the samples was calculated according to the equation below:

$$SR = (W_t - W_o) / W_o \quad (1)$$

**Table 1.** Composition of the Fabricated Oxygen Generating Hydrogels

	hydrogel GelMA (mg)	calcium peroxide (CPO) (mg)	DMSO (mL)
0% CPO-GelMA	200	0	4
1% CPO-GelMA	200	2	4
2% CPO-GelMA	200	4	4
3% CPO-GelMA	200	6	4

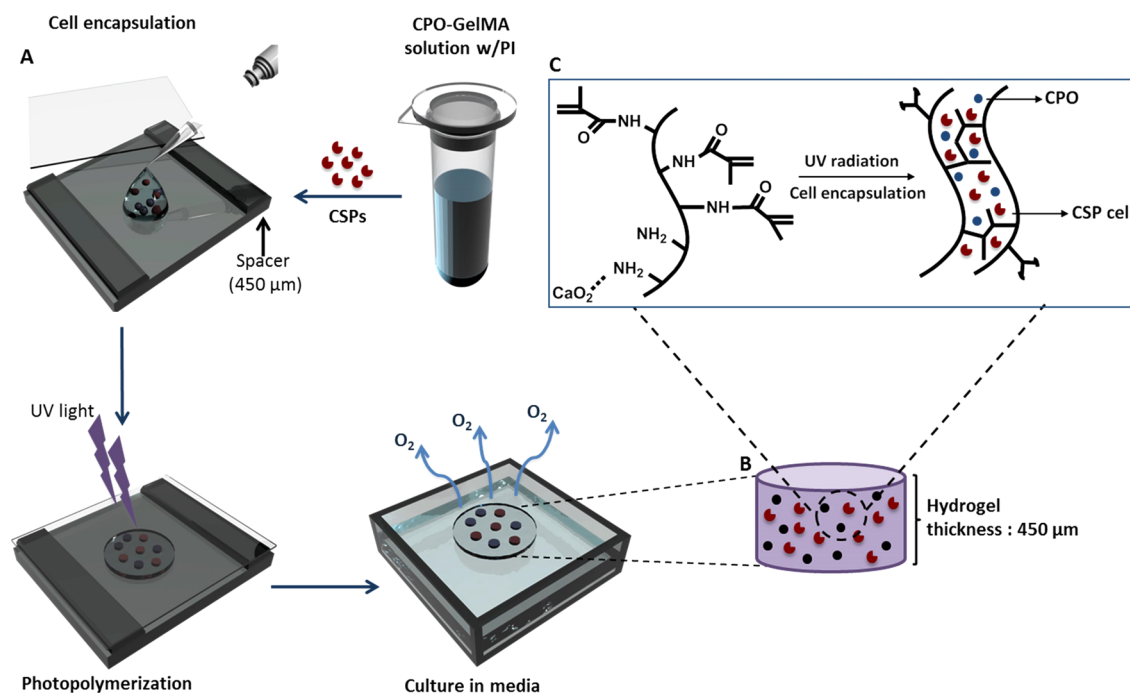


**Figure 1.** Schematic design of the fabrication of CPO-based oxygen-generating GelMA hydrogels. (A) CPO-GelMA is mixed with CSPs and placed in a geometrically defined mold after which the mixture is cross-linked into a hydrogel construct using UV light. (B) Schematic representation of the resulting 450  $\mu\text{m}$  high CPO-GelMA hydrogel and (C) its chemical structure.

Here,  $W_i$  and  $W_o$  are the weights of the swollen and dried samples, respectively.

**Oxygen Release Kinetics of CPO-GelMA Hydrogels.** Oxygen release kinetics of CPO-GelMA hydrogels was determined by using a ruthenium complex oxygen sensor (Ocean Optics, NeoFox System) under hypoxic conditions. For measurement of dissolved oxygen (DO), GelMA-only and CPO-GelMA hydrogels including different amounts of CPO were individually placed into 12-well plates containing 3 mL of medium with catalase (100U/mL) in each well and placed in a 1%  $\text{O}_2$  incubator.

**Cell Encapsulation within Oxygen-Generating Hydrogels.** CSPs were dispersed into the DPBS solution containing 0.1% (w/v) photoinitiator (Irgacure 2959) and 5% (w/v) CPO-GelMA with different concentrations of CPO (0, 1, 2, and 3 wt % CPO) with a cell density of  $5 \times 10^6$  cells/mL. The prepared cell solution (30  $\mu\text{L}$ ) was added dropwise on 3-(trimethoxysilyl)propyl methacrylate coated glass and cross-linked (Figure 1A–C). Encapsulated CSPs were cultured in Alpha-MEM containing 25% HyClone Characterized FBS, 500U/mL penicillin, 500  $\mu\text{g}/\text{mL}$  streptomycin, 112.5 mg/L L-glutamine, and 100 U/mL catalase for up to 5 days under hypoxic (1%  $\text{O}_2$ , 5%  $\text{CO}_2$ , and 94%  $\text{N}_2$ ) or normoxic conditions (21%  $\text{O}_2$ , 5%  $\text{CO}_2$ , and 74%  $\text{N}_2$ ).

**Cell Metabolic Activity in Oxygen-Generating Hydrogels.** The effect of oxygen-generating hydrogels on the encapsulated cells' metabolic activity was determined using a colorimetric MTS assay. For this assay, MTS solution was prepared by adding 0.2 mL of MTS per 1 mL of colorless Dulbecco's modified Eagle's medium (DMEM, Gibco, USA). CPO-GelMA containing CSPs were cultured for 3 or 5 days under hypoxic conditions, washed three times with DPBS, and placed into new 24-well culture plates. Following this, 400  $\mu\text{L}$  of MTS solution was added to each sample. After incubation for 4 h at 37  $^\circ\text{C}$  under light free conditions, 100  $\mu\text{L}$  of sodium dodecyl sulfate (10%) was added to each sample and incubated overnight under the same conditions. The absorbance value of the solution of 100  $\mu\text{L}$  for each sample was measured using a microplate reader at 490 nm. The obtained absorbance values were normalized to the absorbance values at day 0.

**Cell Survival in CPO-GelMA Hydrogels.** CSP viability in CPO-GelMA hydrogels was evaluated by a live/dead assay. Three samples for each condition were stained with live/dead assay (Invitrogen, USA) according to the manufacturer's instructions. Moreover, the presence

of healthy, apoptotic, and necrotic cells cultured within CPO-GelMA hydrogels under hypoxic conditions were determined using the apoptotic/necrotic cells detection kit (PromoKine, USA) following the manufacturer's instructions. This stained the healthy, apoptotic, and necrotic cells blue, green, and red, respectively. Stained cells were imaged using a confocal microscope (Nikon Instruments, Inc. A1/C1 Confocal Microscope). High-resolution image-stacks were obtained with 10  $\mu\text{m}$  separations between slices (z-stacks). The images of three different representative sections for each sample were collected. Stained cells were quantified using ImageJ software.

**Lactate Dehydrogenase (LDH) Release by CSPs in CPO-GelMA.** The cell damaging effects of hypoxic conditions were assessed by quantifying LDH, which is released by damaged cells. Briefly, incubation media of CSPs encapsulated within CPO-GelMA hydrogels was collected after culture and stored at  $-20$   $^\circ\text{C}$  until measured. The LDH quantification was performed according to the manufacturer's instructions using a COBAS 6000 immunochemistry analyzer (Roche Diagnostics, Indianapolis, IN).

**Statistical Analyses.** Statistical differences between distinct groups were analyzed using one-way ANOVA. To determine whether there were significant differences in the data, Bonferroni post-hoc test was utilized as a comparison test. Statistical significance was set to  $P < 0.05$ ,  $< 0.01$ , and  $< 0.001$  and was indicated with single, double, or triple asterisks, respectively. All results are presented as the mean  $\pm$  standard deviation (SD). All experiments were performed with 5 biological replicates.

## RESULTS AND DISCUSSION

**Fabrication and Characterization of Oxygen-Generating Hydrogels.** Sufficient oxygen availability is essential for cell survival, differentiation, and function in tissue engineering applications.<sup>40–44</sup> Specifically, oxygen availability is particularly challenging in the case of myocardial infarction.<sup>45,46</sup> The infarcted ischemic myocardial tissue presents a hostile micro-environment for implanted cells. In order to enhance viability and mitigate hypoxia-induced cell death of implanted cells, we fabricated an oxygen-generating hydrogel by incorporating CPO particles, which were aggregates of 2  $\mu\text{m}$  with a standard



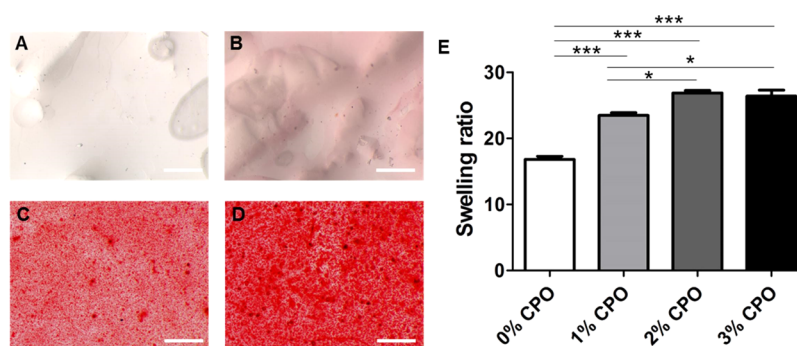


**Figure 2.** Calcium peroxide distribution within CPO-GelMA hydrogels. Microphotographs of Alizarin Red S stained (A) 0% CPO-GelMA, (B) 1% CPO-GelMA, (C) 2% CPO-GelMA, or (D) 3% CPO-GelMA. (E) Swelling ratio of the CPO-GelMA hydrogels containing different concentrations of CPO. Scale bars equal 50  $\mu$ m.

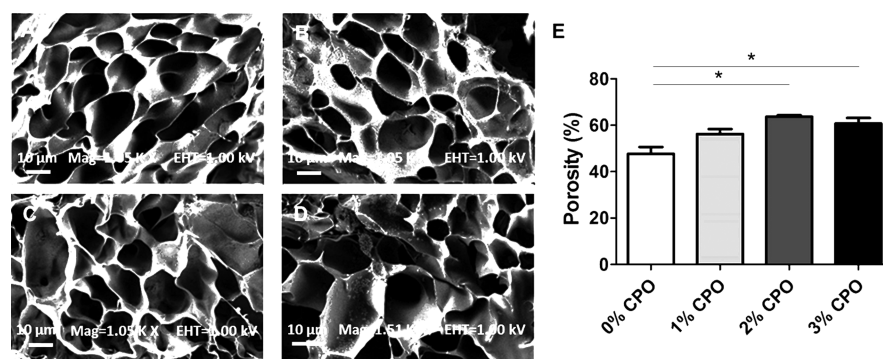


**Figure 3.** Effect of CPO on GelMA hydrogels' porosity. SEM images for cross-section and inner pore structure of GelMA hydrogels containing (A) 0% CPO, (B) 1% CPO, (C) 2% CPO, or (D) 3% CPO. (E) Semi-quantitation of GelMA hydrogel porosity based on image analysis.

deviation of 1.1  $\mu$ m, into GelMA hydrogels (Figure 1A–C). GelMA is a cytocompatible and degradable hydrogel that mimics 3D native tissue constructs and provides a natural and mechanically protective environment for encapsulated cells. Hydrogels having such porous structures have been applied efficiently because of their hydrophilic properties, which aid in maintaining cardiac cell viability and function of engineered cardiac tissues.<sup>47</sup>

To demonstrate that CPO particles were successfully and homogeneously incorporated into the GelMA structure, all of the samples containing different amounts of CPO (0, 1, 2, and 3%) were stained by Alizarin Red S (Figure 2A–D). Alizarin Red S reacts with calcium via its sulfonic acid and/or its OH groups and thereby visualizes inorganic calcium as a red stain. The staining intensity increased with increasing CPO-GelMA concentrations, confirming that CPO was efficiently incorporated into the GelMA hydrogel. Moreover, CPO particles were homogeneously dispersed throughout the entire GelMA hydrogel, which is vital for spatiotemporally predictable and controllable oxygen generation.

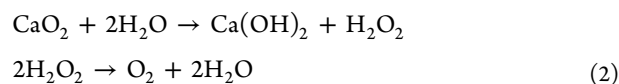
Next, we determined the effect of CPO on the swelling GelMA hydrogels (Figure 2E). The swelling ratio of CPO-based GelMA hydrogels increased with increasing CPO concentration. The swelling ratio of GelMA hydrogels increased from  $\sim 17 \pm 0.8$  up to  $\sim 27 \pm 0.7$  upon incorporation of 3% CPO. These results agree with expectations since (i) the incorporation of solid peroxide particles increases the water permeability<sup>48</sup> and (ii) the cross-linking density determines the hydrogel's swelling properties as well as its porosity.<sup>49</sup>

Porosity is one of the most important features for biomaterials, especially in tissue engineering applications as it is related to

the swelling capacity of biomaterials. SEM images were taken to observe the effect of CPO incorporation on the structure (porosity) of the hydrogel (Figure 3A–D). SEM analysis demonstrated a small but significant increase in porosity upon increasing the CPO concentration in the GelMA hydrogels. This minor increase might be caused by the light blocking effect of CPO particles during UV cross-linking. This would decrease the hydrogel's cross-link density and thus increased porosity (Figure 3E). Therefore, the change in porosity might be unique to light curable hydrogels and allow for even further fine-tuned porosities in this type of biomaterials.

### 3.2. Oxygen Release Kinetics of CPO-GelMA Hydrogels.

Solid peroxides such as CPO are well known for their capability to controllably generate and release oxygen upon contacting water. The reaction of CPO with water is given below (eq 2):



To determine the oxygen release kinetics of CPO-GelMA, hydrogels containing different amounts of CPO (0, 1, 2, or 3%) were individually placed into a 12-well plate containing 3 mL of medium and catalase. Subsequently, the media's dissolved oxygen was measured using an oxygen sensor for 5 days. Measurements were performed under hypoxic conditions within a sealed hypoxia box that was continuously flushed with pure nitrogen gas. As expected, GelMA without CPO remained at  $\sim 0\%$   $\text{O}_2$  throughout the entire experiment (Figure 4). This confirmed that there was no significant amount of dissolved oxygen initially present in both the medium and the hydrogel. Moreover, it underlined that GelMA by itself could not generate oxygen. In contrast, CPO containing GelMA hydrogels provided sustained release of

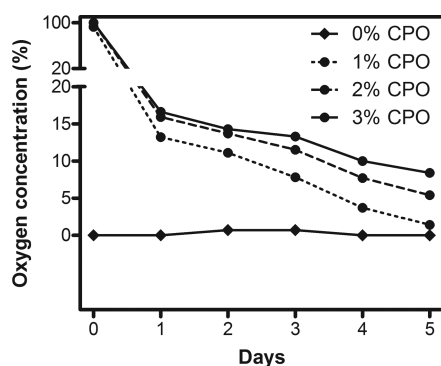


**Figure 4.** Oxygen release kinetics of 0, 1, 2, or 3% CPO-GelMA hydrogels under anoxic conditions.

oxygen for at least 5 days. An immediate bulk release of oxygen increased the oxygen concentration up to 100% upon encapsulation in the aqueous environment of the hydrogel. Despite the quick bulk release, 3% of CPO was able to raise the oxygen tension to  $\sim 17\%$  after 1 day,  $\sim 13\%$  after 3 days, and  $\sim 8\%$  after 5 days. CPO was able to increase the oxygen tension in a dose-dependent manner; 2% and 1% of CPO raised the oxygen tension to  $\sim 5\%$  and  $\sim 1.5\%$  after 5 days, respectively. This release curve can be attributed to the fast paced reaction speed of CPO, which

rapidly decreases the amounts of CPO able to generate oxygen. Regardless, CPO-GelMA was capable of providing an oxygen enriched microenvironment for at least 5 days.

**Enhanced CSP Viability in Oxygen-Generating Hydrogel under Hypoxic Conditions.** To demonstrate the functionality of the oxygen-generating hydrogels, CSPs were encapsulated within CPO-GelMA containing varying concentrations of CPO ranging from 0 to 3% and cultured for up to 5 days. The metabolic activity of CSPs significantly decreases when cultured under hypoxia as compared to normoxia (Figure 5). The metabolic activity of CSPs in CPO-GelMA cultured under hypoxic conditions restored to nonhypoxic levels in a CPO dose-dependent manner. In fact, by incorporating at least 2% CPO in GelMA, the metabolic activities of CSPs cultured under 1%  $O_2$  conditions became indistinguishable from those cultured under 21%  $O_2$  conditions. This suggested that the detrimental effects of an ischemic microenvironment can be avoided by incorporating CPO in GelMA, at least for a period of 5 days. This significantly widens the time frame in which the implant can remain viable to allow for vascular invasion.

To determine CPO-GelMA's oxygen-generating effect on cell survival, the amount of live or dead cells was visualized (Figure 6A and Supporting Information, Figure 1) and quantified (Figure 6B). CSP survival in CPO-GelMA corroborated with

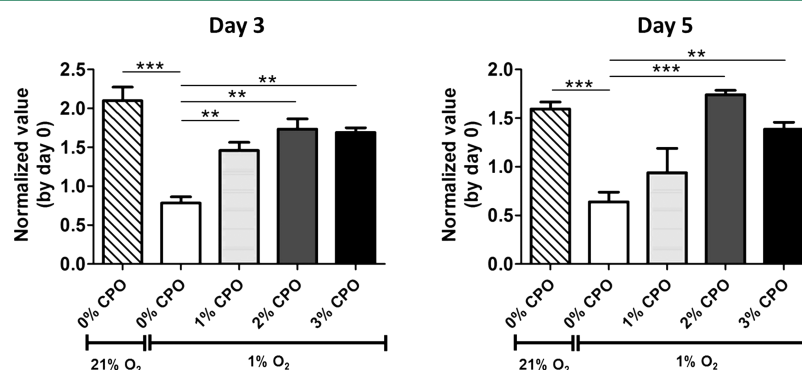


**Figure 5.** CPO-GelMA increases the metabolic activity of CSPs cultured under hypoxic conditions to near normoxic levels. Obtained values were normalized to day 0.

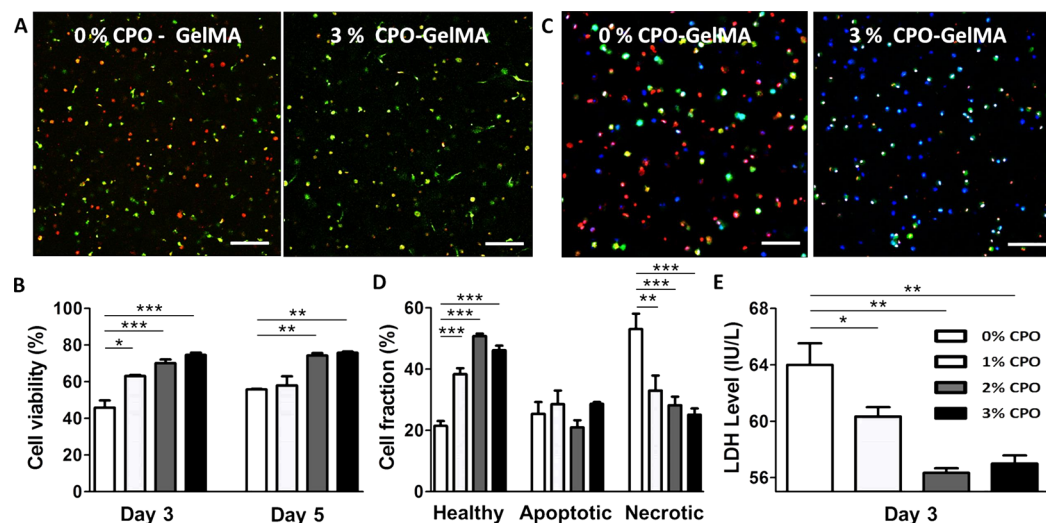


**Figure 6.** CPO-GelMA increases the survival of CSPs by preventing hypoxia induced necrosis. Confocal microphotographs and semi quantification of (A,B) live (green)/dead (red) and (C,D) healthy (blue), apoptotic (green), and necrotic (red) CSPs cultured under hypoxic conditions in CPO-GelMA containing 0, 1, 2, or 3% CPO. (E) Extracellular LDH activity of CSP cultured within CPO-GelMA. Scale bar equals 50  $\mu m$ .

the metabolic activity as the incorporation of CPO significantly improved cell survival. CSPs in GelMA under hypoxia underwent significant amounts of cell death with as little as ~45% surviving cells. In remarkable contrast, CPO-GelMA demonstrated cell survival rates of up to ~80%. It is noteworthy that this remarkable difference in cell survival was maintained for at least 5 days under ischemic conditions.

Hypoxia-induced cell death of cardiac cells can be mediated via either necrosis or apoptosis. Specifically, while apoptosis is undesirable, necrosis is disastrous due to its inherent capacity to inflict damage to surrounding cells and tissues. We determined that CSPs in GelMA without oxygen generation are approximately twice as likely to die of necrosis ( $53.1 \pm 8.7\%$ ) than of apoptosis ( $25.4 \pm 6.7\%$ ) (Figure 6C–D and Supporting Information, Figure 2). Strikingly, the addition of CPO to GelMA improves CSP survival by strongly reducing the amount of necrosis but not apoptosis. Specifically, the addition of 3% CPO to GelMA reduces the necrotic cell fraction to  $25.1 \pm 3.6\%$ . Indeed, the CPO-based decrease in necrotic CSPs was directly mirrored in the increase in surviving healthy CSPs.

To corroborate our surprising oxygen-generation-based decrease in necrosis, CSPs' excretion of lactate dehydrogenase (LDH) was quantified (Figure 6E). Necrosis is characterized by plasma membrane rupture, which will increase the extracellular LDH activity.<sup>50–52</sup> Indeed, CSPs encapsulated within CPO-GelMA demonstrated a CPO-dose-dependent decline in excreted LDH level with a maximal effect from 2% of CPO onward.

Together, these results suggest that oxygen generation using CPO reduces the amount of cell death in cell laden hydrogels. Specifically, we have shown that CPO can reduce hypoxia-induced necrosis of CSPs by increasing oxygen availability under conditions that mimic an infarcted heart. Reduction of cell necrosis is an important feat as this form of uncontrolled cell death irrevocably causes damage to surrounding cells and tissues, which can result in the formation of a sterile inflammatory response<sup>53</sup> and thus implant failure. Therefore, the oxygen-generating properties of CPO-GelMA is expected to improve tissue engineered strategies not only by augmented cell and tissue survival by amelioration of hypoxic stress but also through reduction of necrosis-induced cell and tissue damage.

## CONCLUSIONS

Oxygen-generating hydrogels were fabricated by incorporating varying concentrations of CPO in GelMA. CPO significantly increased the survival and growth of CSPs encapsulated in GelMA hydrogel by alleviating the otherwise occurring hypoxic stress. The most important finding of this study is that CPO-based oxygen generation reduced hypoxia-induced cell death by limiting the necrosis. In short, CPO-based oxygen-generating hydrogels can potentially improve the viability of cardiac cells and minimize cell loss in infarcted myocardial tissue. Therefore, oxygen-generating hydrogels such as CPO-GelMA have the potential to improve tissue engineering strategies that aim to regenerate ischemic tissues.

## ASSOCIATED CONTENT

### Supporting Information

Supplemental Figure 1: Confocal microphotographs of live/dead stained CSPs cultured in CPO-GelMA containing 0, 1, 2, or 3% CPO under hypoxic conditions for three or 5 days. Live or dead cells are stained green or red, respectively. Scale bar equals 50  $\mu\text{m}$ . Supplemental Figure 2: Confocal microphotographs of healthy, apoptotic, and necrotic CSPs cultured in CPO-GelMA

containing 0, 1, 2, or 3% CPO under hypoxic conditions. Healthy, apoptotic, and necrotic cells stained blue, green and red, respectively. Scale bar equals 50  $\mu\text{m}$ . The Supporting Information is available free of charge on the ACS Publications website at DOI: 10.1021/acsbiomaterials.6b00109.

(PDF)

## AUTHOR INFORMATION

### Corresponding Author

\*E-mail: [alik@bwh.harvard.edu](mailto:alik@bwh.harvard.edu).

### Notes

The authors declare no competing financial interest.

<sup>^</sup>Harvard University, Department of Chemistry and Chemical Biology, 12 Oxford Street, Cambridge, MA 02138, USA

<sup>§</sup>Marmara University, Department of Chemical Engineering, 34722, Istanbul, Turkey

<sup>♦</sup>Department of Biomedical Engineering, Texas A&M University, College Station, Texas 77843, United States

## ACKNOWLEDGMENTS

We acknowledge funding from the National Science Foundation (EFRI-1240443), IMMODGEL (602694), and the National Institutes of Health (EB012597, AR057837, DE021468, HL099073, AI105024, and AR063745). J.L. acknowledges financial support from Innovative Research Incentives Scheme Veni #14328 of The Netherlands Organization for Scientific Research (NWO).

## REFERENCES

- (1) Olivetti, G.; Abbi, R.; Quaini, F.; Kajstura, J.; Cheng, W.; Nitahara, J. A.; Quaini, E.; Di Loreto, C.; Beltrami, C. A.; Krajewski, S.; Reed, J. C.; Anversa, P. Apoptosis in the failing human heart. *N. Engl. J. Med.* **1997**, *336* (16), 1131–41.
- (2) Aguirre, A.; Sancho-Martinez, I.; Izpisua Belmonte, J. C. Reprogramming toward heart regeneration: stem cells and beyond. *Cell stem cell* **2013**, *12* (3), 275–84.
- (3) Soh, B. S.; Wu, H.; Chien, K. R. Cardiac regenerative medicine 2.0. *Nat. Biotechnol.* **2013**, *31* (3), 209–11.
- (4) Pfister, O.; Mouquet, F.; Jain, M.; Summer, R.; Helmes, M.; Fine, A.; Colucci, W. S.; Liao, R. CD31- but Not CD31+ cardiac side population cells exhibit functional cardiomyogenic differentiation. *Circulation research* **2005**, *97* (1), 52–61.
- (5) Bauer, M.; Kang, L.; Qiu, Y.; Wu, J.; Peng, M.; Chen, H. H.; Camci-Unal, G.; Bayomy, A. F.; Sosnovik, D. E.; Khademhosseini, A.; Liao, R. Adult cardiac progenitor cell aggregates exhibit survival benefit both in vitro and in vivo. *PLoS One* **2012**, *7* (11), e50491.
- (6) Unno, K.; Jain, M.; Liao, R. Cardiac side population cells: moving toward the center stage in cardiac regeneration. *Circ. Res.* **2012**, *110* (10), 1355–63.
- (7) Wu, J. C.; Chen, I. Y.; Sundaresan, G.; Min, J. J.; De, A.; Qiao, J. H.; Fishbein, M. C.; Gambhir, S. S. Molecular imaging of cardiac cell transplantation in living animals using optical bioluminescence and positron emission tomography. *Circulation* **2003**, *108* (11), 1302–5.
- (8) Paul, A.; Ge, Y.; Prakash, S.; Shum-Tim, D. Microencapsulated stem cells for tissue repairing: implications in cell-based myocardial therapy. *Regener. Med.* **2009**, *4* (5), 733–45.
- (9) Penicka, M.; Widimsky, P.; Kobylka, P.; Kozak, T.; Lang, O. Images in cardiovascular medicine. Early tissue distribution of bone marrow mononuclear cells after transcatheter transplantation in a patient with acute myocardial infarction. *Circulation* **2005**, *112* (4), e63–5.
- (10) Haider, H.; Ashraf, M. Strategies to promote donor cell survival: combining preconditioning approach with stem cell transplantation. *J. Mol. Cell. Cardiol.* **2008**, *45* (4), 554–66.
- (11) Wu, K. H.; Mo, X. M.; Han, Z. C.; Zhou, B. Stem cell engraftment and survival in the ischemic heart. *Annals of thoracic surgery* **2011**, *92* (5), 1917–25.



- (12) Zhang, H.; Chen, H.; Wang, W.; Wei, Y.; Hu, S. Cell survival and redistribution after transplantation into damaged myocardium. *J. Cell. Mol. Med.* **2010**, *14* (5), 1078–82.
- (13) Al Kindi, A. H.; Asenjo, J. F.; Ge, Y.; Chen, G. Y.; Bhathena, J.; Chiu, R. C.; Prakash, S.; Shum-Tim, D. Microencapsulation to reduce mechanical loss of microspheres: implications in myocardial cell therapy. *European journal of cardio-thoracic surgery: official journal of the European Association for Cardio-thoracic Surgery* **2011**, *39* (2), 241–7.
- (14) Leijten, J.; Khademhosseini, A. From Nano to Macro: Multiscale Materials for Improved Stem Cell Culturing and Analysis. *Cell stem cell* **2016**, *18* (1), 20–4.
- (15) Paul, A.; Shao, W.; Abbasi, S.; Shum-Tim, D.; Prakash, S. PAMAM dendrimer-baculovirus nanocomplex for microencapsulated adipose stem cell-gene therapy: in vitro and in vivo functional assessment. *Mol. Pharmaceutics* **2012**, *9* (9), 2479–88.
- (16) Lan, F.; Liu, J.; Narsinh, K. H.; Hu, S.; Han, L.; Lee, A. S.; Karow, M.; Nguyen, P. K.; Nag, D.; Calos, M. P.; Robbins, R. C.; Wu, J. C. Safe genetic modification of cardiac stem cells using a site-specific integration technique. *Circulation* **2012**, *126* (11 Suppl 1), S20–8.
- (17) Lu, G.; Haider, H. K.; Jiang, S.; Ashraf, M. Sca-1+ stem cell survival and engraftment in the infarcted heart: dual role for preconditioning-induced connexin-43. *Circulation* **2009**, *119* (19), 2587–96.
- (18) Tang, Y. L.; Zhu, W.; Cheng, M.; Chen, L.; Zhang, J.; Sun, T.; Kishore, R.; Phillips, M. I.; Losordo, D. W.; Qin, G. Hypoxic preconditioning enhances the benefit of cardiac progenitor cell therapy for treatment of myocardial infarction by inducing CXCR4 expression. *Circ. Res.* **2009**, *104* (10), 1209–16.
- (19) Paul, A.; Chen, G.; Khan, A.; Rao, V. T.; Shum-Tim, D.; Prakash, S. Genipin-cross-linked microencapsulated human adipose stem cells augment transplant retention resulting in attenuation of chronically infarcted rat heart fibrosis and cardiac dysfunction. *Cell transplantation* **2012**, *21* (12), 2735–51.
- (20) Danoviz, M. E.; Nakamuta, J. S.; Marques, F. L.; dos Santos, L.; Alvarenga, E. C.; dos Santos, A. A.; Antonio, E. L.; Schetter, I. T.; Tucci, P. J.; Krieger, J. E. Rat adipose tissue-derived stem cells transplantation attenuates cardiac dysfunction post infarction and biopolymers enhance cell retention. *PLoS One* **2010**, *5* (8), e12077.
- (21) Shin, S. R.; Jung, S. M.; Zalabany, M.; Kim, K.; Zorlutuna, P.; Kim, S. B.; Nikkhah, M.; Khabiry, M.; Azize, M.; Kong, J.; Wan, K. T.; Palacios, T.; Dokmeci, M. R.; Bae, H.; Tang, X. S.; Khademhosseini, A. Carbon-nanotube-embedded hydrogel sheets for engineering cardiac constructs and bioactuators. *ACS Nano* **2013**, *7* (3), 2369–80.
- (22) Shin, S. R.; Bae, H.; Cha, J. M.; Mun, J. Y.; Chen, Y. C.; Tekin, H.; Shin, H.; Farshchi, S.; Dokmeci, M. R.; Tang, S.; Khademhosseini, A. Carbon nanotube reinforced hybrid microgels as scaffold materials for cell encapsulation. *ACS Nano* **2012**, *6* (1), 362–72.
- (23) Zhang, D.; Shadrin, I. Y.; Lam, J.; Xian, H. Q.; Snodgrass, H. R.; Bursac, N. Tissue-engineered cardiac patch for advanced functional maturation of human ESC-derived cardiomyocytes. *Biomaterials* **2013**, *34* (23), 5813–20.
- (24) Seif-Naraghi, S. B.; Singelyn, J. M.; Salvatore, M. A.; Osborn, K. G.; Wang, J. J.; Sampat, U.; Kwan, O. L.; Strachan, G. M.; Wong, J.; Schup-Magoffin, P. J.; Braden, R. L.; Bartels, K.; DeQuach, J. A.; Preul, M.; Kinsey, A. M.; DeMaria, A. N.; Dib, N.; Christman, K. L. Safety and efficacy of an injectable extracellular matrix hydrogel for treating myocardial infarction. *Sci. Transl. Med.* **2013**, *5* (173), 173ra25.
- (25) Bae, H.; Puranik, A. S.; Gauvin, R.; Edalat, F.; Carrillo-Conde, B.; Peppas, N. A.; Khademhosseini, A. Building vascular networks. *Sci. Transl. Med.* **2012**, *4* (160), 160ps23.
- (26) Yu, J.; Du, K. T.; Fang, Q.; Gu, Y.; Mihardja, S. S.; Sievers, R. E.; Wu, J. C.; Lee, R. J. The use of human mesenchymal stem cells encapsulated in RGD modified alginate microspheres in the repair of myocardial infarction in the rat. *Biomaterials* **2010**, *31* (27), 7012–20.
- (27) Paul, A.; Hasan, A.; Kindi, H. A.; Gaharwar, A. K.; Rao, V. T.; Nikkhah, M.; Shin, S. R.; Krafft, D.; Dokmeci, M. R.; Shum-Tim, D.; Khademhosseini, A. Injectable graphene oxide/hydrogel-based angiogenic gene delivery system for vasculogenesis and cardiac repair. *ACS Nano* **2014**, *8* (8), 8050–62.
- (28) Camci-Unal, G.; Alemdar, N.; Annabi, N.; Khademhosseini, A. Oxygen Releasing Biomaterials for Tissue Engineering. *Polym. Int.* **2013**, *62* (6), 843–848.
- (29) Leijten, J.; Georgi, N.; Moreira Teixeira, L.; van Blitterswijk, C. A.; Post, J. N.; Karperien, M. Metabolic programming of mesenchymal stromal cells by oxygen tension directs chondrogenic cell fate. *Proc. Natl. Acad. Sci. U.S.A.* **2014**, *111*, 13954–13959.
- (30) Harrison, B. S.; Eberli, D.; Lee, S. J.; Atala, A.; Yoo, J. J. Oxygen producing biomaterials for tissue regeneration. *Biomaterials* **2007**, *28* (31), 4628–34.
- (31) Oh, S. H.; Ward, C. L.; Atala, A.; Yoo, J. J.; Harrison, B. S. Oxygen generating scaffolds for enhancing engineered tissue survival. *Biomaterials* **2009**, *30* (5), 757–62.
- (32) Li, Z.; Guo, X.; Guan, J. An oxygen release system to augment cardiac progenitor cell survival and differentiation under hypoxic condition. *Biomaterials* **2012**, *33* (25), 5914–23.
- (33) Pedraza, E.; Coronel, M. M.; Fraker, C. A.; Ricordi, C.; Stabler, C. L. Preventing hypoxia-induced cell death in beta cells and islets via hydrolytically activated, oxygen-generating biomaterials. *Proc. Natl. Acad. Sci. U. S. A.* **2012**, *109* (11), 4245–50.
- (34) Nichol, J. W.; Koshy, S. T.; Bae, H.; Hwang, C. M.; Yamanlar, S.; Khademhosseini, A. Cell-laden microengineered gelatin methacrylate hydrogels. *Biomaterials* **2010**, *31* (21), 5536–44.
- (35) Shin, H.; Olsen, B. D.; Khademhosseini, A. The mechanical properties and cytotoxicity of cell-laden double-network hydrogels based on photocrosslinkable gelatin and gellan gum biomacromolecules. *Biomaterials* **2012**, *33* (11), 3143–52.
- (36) Camci-Unal, G.; Cuttica, D.; Annabi, N.; Demarchi, D.; Khademhosseini, A. Synthesis and characterization of hybrid hyaluronic acid-gelatin hydrogels. *Biomacromolecules* **2013**, *14* (4), 1085–92.
- (37) Hosseini, V.; Ahadian, S.; Ostrovidov, S.; Camci-Unal, G.; Chen, S.; Kaji, H.; Ramalingam, M.; Khademhosseini, A. Engineered contractile skeletal muscle tissue on a microgrooved methacrylated gelatin substrate. *Tissue Eng., Part A* **2012**, *18* (23–24), 2453–65.
- (38) Khademhosseini, A.; Langer, R.; Borenstein, J.; Vacanti, J. P. Microscale technologies for tissue engineering and biology. *Proc. Natl. Acad. Sci. U. S. A.* **2006**, *103* (8), 2480–7.
- (39) Qi, H.; Du, Y.; Wang, L.; Kaji, H.; Bae, H.; Khademhosseini, A. Patterned differentiation of individual embryoid bodies in spatially organized 3D hybrid microgels. *Adv. Mater.* **2010**, *22* (46), 5276–81.
- (40) Carrier, R. L.; Papadaki, M.; Rupnick, M.; Schoen, F. J.; Bursac, N.; Langer, R.; Freed, L. E.; Vunjak-Novakovic, G. Cardiac tissue engineering: cell seeding, cultivation parameters, and tissue construct characterization. *Biotechnol. Bioeng.* **1999**, *64* (5), 580–9.
- (41) Lewis, M. C.; Macarthur, B. D.; Malda, J.; Pettet, G.; Please, C. P. Heterogeneous proliferation within engineered cartilaginous tissue: the role of oxygen tension. *Biotechnol. Bioeng.* **2005**, *91* (5), 607–15.
- (42) Radisic, M.; Yang, L.; Boublik, J.; Cohen, R. J.; Langer, R.; Freed, L. E.; Vunjak-Novakovic, G. Medium perfusion enables engineering of compact and contractile cardiac tissue. *Am. J. Physiol. Heart Circ. Physiol.* **2004**, *286* (2), H507–16.
- (43) Leijten, J. C.; Moreira Teixeira, L. S.; Landman, E. B.; van Blitterswijk, C. A.; Karperien, M. Hypoxia inhibits hypertrophic differentiation and endochondral ossification in explanted tibiae. *PLoS One* **2012**, *7* (11), e49896.
- (44) Leijten, J.; Chai, Y. C.; Papantoniou, I.; Geris, L.; Schrooten, J.; Luyten, F. P. Cell based advanced therapeutic medicinal products for bone repair: Keep it simple? *Advanced drug delivery reviews* **2015**, *84*, 30–44.
- (45) Robey, T. E.; Saiget, M. K.; Reinecke, H.; Murry, C. E. Systems approaches to preventing transplanted cell death in cardiac repair. *J. Mol. Cell. Cardiol.* **2008**, *45* (4), 567–81.
- (46) Lairet, K. F.; Baer, D.; Leas, M. L.; Renz, E. M.; Cancio, L. C. Evaluation of an oxygen-diffusion dressing for accelerated healing of donor-site wounds. *Journal of burn care & research: official publication of the American Burn Association* **2014**, *35* (3), 214–8.
- (47) Cheng, M.; Park, H.; Engelmayr, G. C.; Moretti, M.; Freed, L. E. Effects of regulatory factors on engineered cardiac tissue in vitro. *Tissue Eng.* **2007**, *13* (11), 2709–19.

- (48) Chen, C.; Wang, J.; Chen, Z. Surface restructuring behavior of various types of poly(dimethylsiloxane) in water detected by SFG. *Langmuir* **2004**, *20* (23), 10186–93.
- (49) Hwang, C. M.; Sant, S.; Masaeli, M.; Kachouie, N. N.; Zamanian, B.; Lee, S. H.; Khademhosseini, A. Fabrication of three-dimensional porous cell-laden hydrogel for tissue engineering. *Biofabrication* **2010**, *2* (3), 035003.
- (50) Schneider, N.; Lejeune, J. P.; Deby, C.; Deby-Dupont, G. P.; Serteyn, D. Viability of equine articular chondrocytes in alginate beads exposed to different oxygen tensions. *Vet. J.* **2004**, *168* (2), 167–73.
- (51) Trubiani, G.; Al Chawaf, A.; Belsham, D. D.; Barsyte-Lovejoy, D.; Lovejoy, D. A. Teneurin carboxy (C)-terminal associated peptide-1 inhibits alkalosis-associated necrotic neuronal death by stimulating superoxide dismutase and catalase activity in immortalized mouse hypothalamic cells. *Brain Res.* **2007**, *1176*, 27–36.
- (52) Zhu, Y.; Shi, Y. P.; Wu, D.; Ji, Y. J.; Wang, X.; Chen, H. L.; Wu, S. S.; Huang, D. J.; Jiang, W. Salidroside protects against hydrogen peroxide-induced injury in cardiac H9c2 cells via PI3K-Akt dependent pathway. *DNA Cell Biol.* **2011**, *30* (10), 809–19.
- (53) Iyer, S. S.; Pulskens, W. P.; Sadler, J. J.; Butter, L. M.; Teske, G. J.; Ulland, T. K.; Eisenbarth, S. C.; Florquin, S.; Flavell, R. A.; Leemans, J. C.; Sutterwala, F. S. Necrotic cells trigger a sterile inflammatory response through the Nlrp3 inflammasome. *Proc. Natl. Acad. Sci. U. S. A.* **2009**, *106* (48), 20388–93.